Elastic and piezoelectric fields in a substrate AlN due to a buried quantum dot

E. Pan[a)]
Department of Civil Engineering, The University of Akron, Akron, Ohio 44325-3905

B. Yang
Materials Reliability Division, National Institute of Standard & Technology, Boulder, Colorado 80305

(Received 13 August 2002; accepted 9 December 2002)

Using the Green's function solution in an anisotropic and linearly piezoelectric half space developed recently by the authors, this article studies the elastic and piezoelectric fields in substrate AlN due to a buried quantum dot (QD). Two different growth orientations are considered: One is the AlN (0001) growing along the (0001) axis, and the other is the AlN (1000) growing along the polar direction [i.e., a direction normal to (0001) axis]. For an InN QD, modeled as a concentrated source, with a volume $v_a = 4\pi R^3/3$ where $R = 3$ nm, and the typical values of misfit strain, at a depth $h = 10$ nm below the surface, the following features have been observed: (1): on the surface of substrate AlN (0001), the hydrostatic strain, piezoelectric potential, and vertical and horizontal electric fields are rotationally symmetric with respect to the z axis. However, these quantities are not rotationally symmetric on the surface of substrate AlN (1000); (2): a hydrostatic strain as large as 0.01 on the surface of the AlN (1000) and as large as 0.008 on the surface of AlN (0001) can be reached, both of which are larger than that on the surface of the substrate GaAs due to a QD with the same volume at the same depth; (3): the piezoelectric potential on the surface of substrate AlN (0001) is much larger than that on the surface of AlN (1000), i.e., 0.8 versus 0.3 V; and (4): large horizontal and vertical electric fields, in the order of 10^8 V/m, can be induced on the surface of AlN, about two orders of magnitude larger than that on the surface of the substrate GaAs due to a QD with the same volume at the same depth. © *2003 American Institute of Physics.*
[DOI: 10.1063/1.1542670]

I. INTRODUCTION

Due to their special electronic and optical features,[1,2] self-assembled quantum dot (QD) structures have attracted great attention in the society of nanoscale science and technology in recent years. QD structures have been fabricated using various semiconductors, such as group III-V and group nitrides. To offer a quantitative explanation for the QD structure through numerical modeling, various computational methods have also been proposed recently. The finite element method and finite difference method, both of which being domain based, have been frequently used.[2–5] Other methods include the two-dimensional Fourier-transform method,[6,7] the atomistic quantum-mechanics model,[8,9] and the Green's-function method.[10] We remark that among the three methods, the Green's-function method is, perhaps, most useful due to its simple, accurate, and efficient features.[10–13] Recently, the authors[14] advanced the Green's-function method to the anisotropic semiconductor substrate by using the point-force Green's-function solutions in an anisotropic and elastic half space.[15]

While the induced elastic field has been extensively studied, only a few works have been carried out on the corresponding piezoelectric field, which appears to be an important factor in determining the electronic and optical properties of the related devices.[1,16] Davies[12] derived the piezoelectric potential induced by a QD in an elastically isotropic and infinite GaAs. Grundmann *et al.*,[2] on the other hand, solved numerically the piezoelectric potential and studied other related electronic and optical properties for the InAs/GaAs pyramidal QDs, using the FDM. Employing a similar approach, Jogai recently calculated the elastic strain in InAs/GaAs QDs[17] and the strain field and piezoelectric polarization charge in the InN/AlN wurtzite QD structure.[18] We remark that the piezoelectric quantities in either InAs/GaAs or InN/AlN were obtained based on a semicoupled piezoelectric model in those works. Recently, Pan[19] proposed a fully coupled model and calculated the QD-induced elastic and piezoelectric fields in both weakly and strongly coupled semiconductors. The results of that article have shown clearly that in strongly electromechanically coupled semiconductors, such as AlN, the semicoupled model could be in serious error and thus the fully coupled model should be used. More recently, based on the fully coupled model, Pan also studied the elastic and piezoelectric fields on the surface of substrates GaAs (001) and GaAs (111),[20] illustrating clearly the importance of the piezoelectric field in the QD modeling.

This article presents some typical elastic and piezoelectric results on the surface of substrate AlN due to a point QD, using the Green's-function solution developed recently by the authors.[19,20] We consider two different growth orientations: One is AlN (0001) growing along the (0001) axis, and

[a)]Electronic mail: pan2@uakron.edu

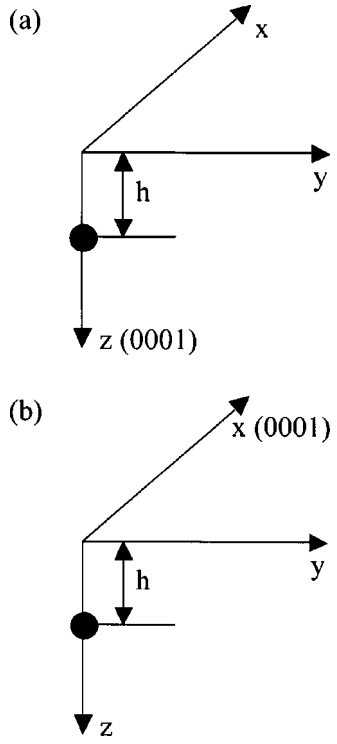

FIG. 1. A buried point quantum dot of volume $v_a = 4\pi R^3/3$ at a depth h below the surface of a half space where $R = 3$ nm and $h = 10$ nm. The misfit strains are $\gamma^*_{xx} = \gamma^*_{yy} = 0.1375$, $\gamma^*_{zz} = 0.1267$ in AlN (0001) in (a), and $\gamma^*_{xx} = 0.1267$, $\gamma^*_{yy} = \gamma^*_{zz} = 0.1375$ in AlN (1000) in (b).

the other is AlN (1000) growing along the polar direction [i.e., a direction normal to (0001) axis]. In Sec. II, the theory is briefly summarized. While benchmark results for the elastic and piezoelectric fields are presented in Sec. III, conclusions are drawn in Sec. IV.

II. THEORY

For a fully coupled piezoelectric semiconductor, the constitutive relations can be expressed as[19–21]

$$\sigma_{ij} = C_{ijlm}\gamma_{lm} - e_{kji}E_k,$$
$$D_i = e_{ijk}\gamma_{jk} + \varepsilon_{ij}E_j, \tag{1}$$

where σ_{ij} and D_i are the stress and electric displacement, respectively; γ_{ij} is the strain and E_i the electric field; C_{ijlm}, e_{ijk}, and ε_{ij} are the elastic moduli, piezoelectric coefficients, and dielectric constants, respectively. It has been shown recently that,[19] for semiconductors with strong electromechanical coupling, such as AlN, Eq. (1) needs to be solved simultaneously.

For an infinitesimal deformation, the elastic strain and electric field are related to the elastic displacement u_i and electric potential ϕ, respectively, as

$$\gamma_{ij} = \tfrac{1}{2}(u_{i,j} + u_{j,i}); \quad E_i = -\phi_{,i}. \tag{2}$$

We now consider a half-space AlN with the x and y axes lying in the traction-free and insulating surface and the z axis pointing towards the interior of AlN [Figs. 1(a) and 1(b)]. Two crystallographic orientations for the substrate will be considered: One with the z axis along the (0001) axis of the AlN crystal [Fig. 1(a)], and the other with the x axis along the (0001) axis [Fig. 1(b)]. For convenience, the former will be named AlN (0001) and the latter AlN (1000). For the substrate with orientation AlN (0001), the material property matrices in Eq. (1) are reduced to

$$[C] = \begin{bmatrix} C_{11} & C_{12} & C_{13} & 0 & 0 & 0 \\ & C_{11} & C_{13} & 0 & 0 & 0 \\ & & C_{33} & 0 & 0 & 0 \\ & & & C_{44} & 0 & 0 \\ & \text{sym} & & & C_{44} & 0 \\ & & & & & C_{66} \end{bmatrix}, \tag{3a}$$

$$[e] = \begin{bmatrix} 0 & 0 & 0 & 0 & e_{15} & 0 \\ 0 & 0 & 0 & e_{15} & 0 & 0 \\ e_{31} & e_{31} & e_{33} & 0 & 0 & 0 \end{bmatrix}, \tag{3b}$$

$$[\varepsilon] = \begin{bmatrix} \varepsilon_{11} & 0 & 0 \\ 0 & \varepsilon_{11} & 0 \\ 0 & 0 & \varepsilon_{33} \end{bmatrix}, \tag{3c}$$

where the material constants are associated with the crystalline coordinates and $C_{66} = (C_{11}\text{-}C_{12})/2$ in Eq. (3a). As is well known, this material belongs to the hexagonal (or transversely isotropic) system C_{6v} (6 mm).[21] We further note that similar expressions for the material property matrices can be found for the substrate with orientation AlN (1000).

At the surface $z = 0$, the traction-free insulating condition, as given below, is assumed

$$\sigma_{xz} = 0; \quad \sigma_{yz} = 0; \quad \sigma_{zz} = 0; \quad D_z = 0 \tag{4}$$

Let us assume that there is an inclusion with eigenstrain (or misfit strain), γ^*_{ij} and E^*_i, of volume v_a at $\boldsymbol{x}$ in the substrate. Our goal is to find the elastic and piezoelectric fields induced by this source. Using the point-force/point-charge Green's-functions and Betti reciprocity theorem, the induced elastic displacement/electric potential, u_k and ϕ, and the elastic strain/electric field, γ_{kj} and E_i, at $\boldsymbol{y}$ can be found, respectively, as[19,20]

$$u_k(\boldsymbol{y}) = [\sigma^k_{ml}(\boldsymbol{x};\boldsymbol{y})\gamma^*_{lm} - D^k_m(\boldsymbol{x};\boldsymbol{y})E^*_m]v_a, \tag{5a}$$

$$\phi(\boldsymbol{y}) = [\sigma^4_{ml}(\boldsymbol{x};\boldsymbol{y})\gamma^*_{lm} - D^4_m(\boldsymbol{x};\boldsymbol{y})E^*_m]v_a, \tag{5b}$$

and

$$\gamma_{kp}(\boldsymbol{y}) = \tfrac{1}{2}\gamma^*_{lm}[\sigma^k_{ml,p_y}(\boldsymbol{x};\boldsymbol{y}) + \sigma^p_{ml,k_y}(\boldsymbol{x};\boldsymbol{y})]v_a$$
$$- \tfrac{1}{2}E^*_m[D^k_{m,p_y}(\boldsymbol{x};\boldsymbol{y}) + D^p_{m,k_y}(\boldsymbol{x};\boldsymbol{y})]v_a, \tag{6a}$$

$$E_p(\boldsymbol{y}) = [E^*_m D^4_{m,p_y}(\boldsymbol{x};\boldsymbol{y}) - \gamma^*_{lm}\sigma^4_{ml,p_y}(\boldsymbol{x};\boldsymbol{y})]v_a, \tag{6b}$$

where the superscripts in Eqs. (5) and (6) indicate the direction of the point force ($k,p = 1,2,3$) and the negative point charge (for superscript 4).[19,20] The quantities with these superscripts are the point-force and point-charge Green's functions described in Pan.[15,19,20] With the elastic strain and electric fields being solved from Eqs. (5) and (6), the stress and electric displacement fields, σ_{ij} and D_i, then can be obtained using Eq. (1).

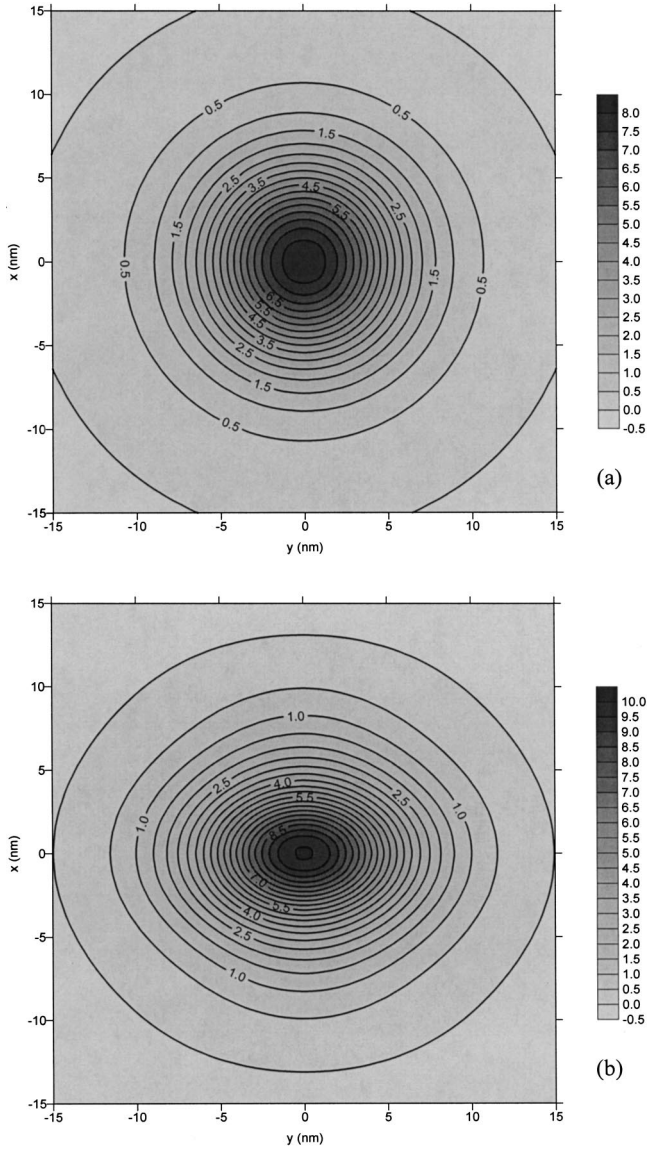

FIG. 2. (a) Contours of the hydrostatic strain $\gamma_{kk}(\times 10^{-3})$ on the surface of AlN (0001) due to a point quantum dot. (b) Contours of the hydrostatic strain γ_{kk} $(\times 10^{-3})$ on the surface of AlN (1000) due to a point quantum dot.

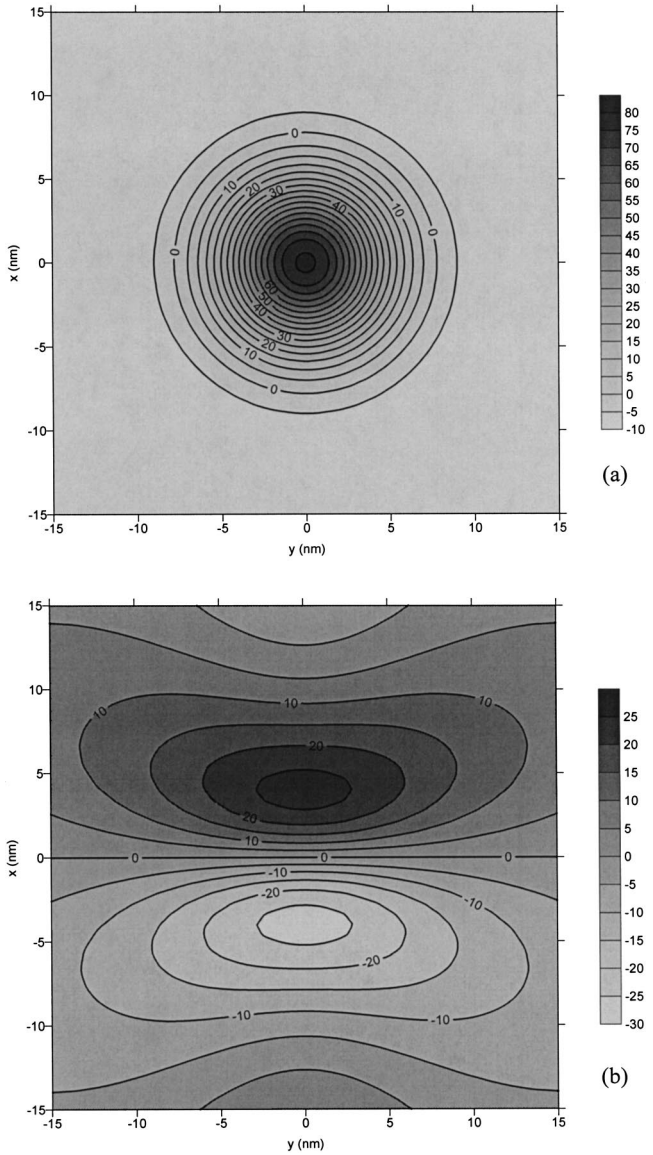

FIG. 3. (a) Contours of the electric potential ϕ $(\times 10^{-2}$ V) on the surface of AlN (0001) due to a point quantum dot. (b) Contours of the electric potential ϕ $(\times 10^{-2}$ V) on the surface of AlN (1000) due to a point quantum dot.

III. RESULTS

The Green's-function solutions (5) and (6) are now applied to the case of a buried InN QD with a volume $v_a = 4\pi R^3/3$ in substrate AlN. The QD is located at a depth h below the surface (Fig. 1) and the misfit strains are given by $\gamma^*_{xx} = \gamma^*_{yy} = 0.1375$ and $\gamma^*_{zz} = 0.1267$ in substrate AlN (0001) [Fig. 1(a)], and $\gamma^*_{xx} = 0.1267$, $\gamma^*_{yy} = \gamma^*_{zz} = 0.1375$ in AlN (1000) [Fig. 1(b)].[16,17] Also in the calculation, R is fixed at 3 nm and h at 10 nm. The material properties for AlN are given in Table I.[16,17]

Shown in Figs. 2(a) and 2(b) are contours of the hydrostatic strain γ_{kk}, respectively, on the surface of substrates AlN (0001) and AlN (1000) due to the buried point QD described above. It is observed that while the distribution of the hydrostatic strain on the surface of substrate AlN (0001) is completely rotationally symmetric about the z axis (i.e., it is independent of the polar angle on the surface), the corresponding contours on the surface of AlN (1000) are in elliptic shape. In other words, the hydrostatic strain on the surface of AlN (1000) has a rotational symmetry of order C_2. Namely, the hydrostatic strain remains the same after a rotation of $2\pi/2$ around the z axis, a feature completely different from that observed previously on the surface of the substrate GaAs.[20] Furthermore, the maximum hydrostatic strains

TABLE I. Material properties for AlN.[16,17] Elastic constants are in GPa, piezoelectric constants in C/m^2, and the dielectric constants are relative to ε_0.

C_{11}	C_{12}	C_{13}	C_{33}	C_{44}
396	137	108	373	116
e_{31}	e_{33}	e_{15}		
-0.58	1.55	-0.48		
ε_{11}	ε_{33}			
9	11			

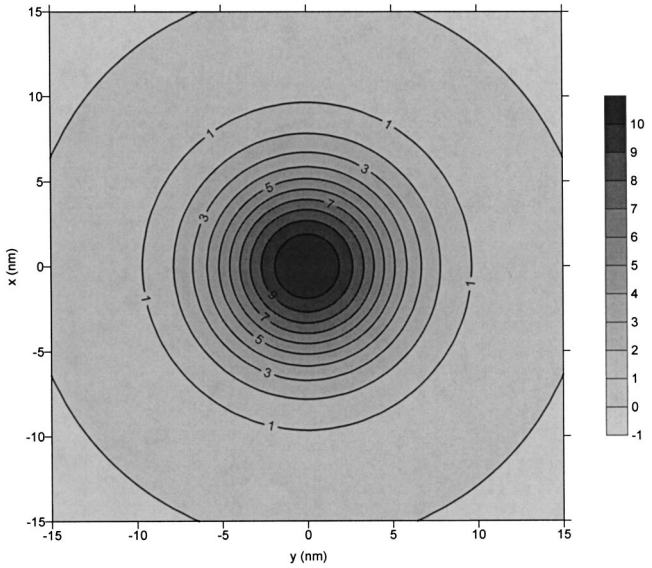

FIG. 4. Contours of the vertical electric field E_z ($\times 10^7$ V/m) on the surface of AlN (0001) due to a point quantum dot.

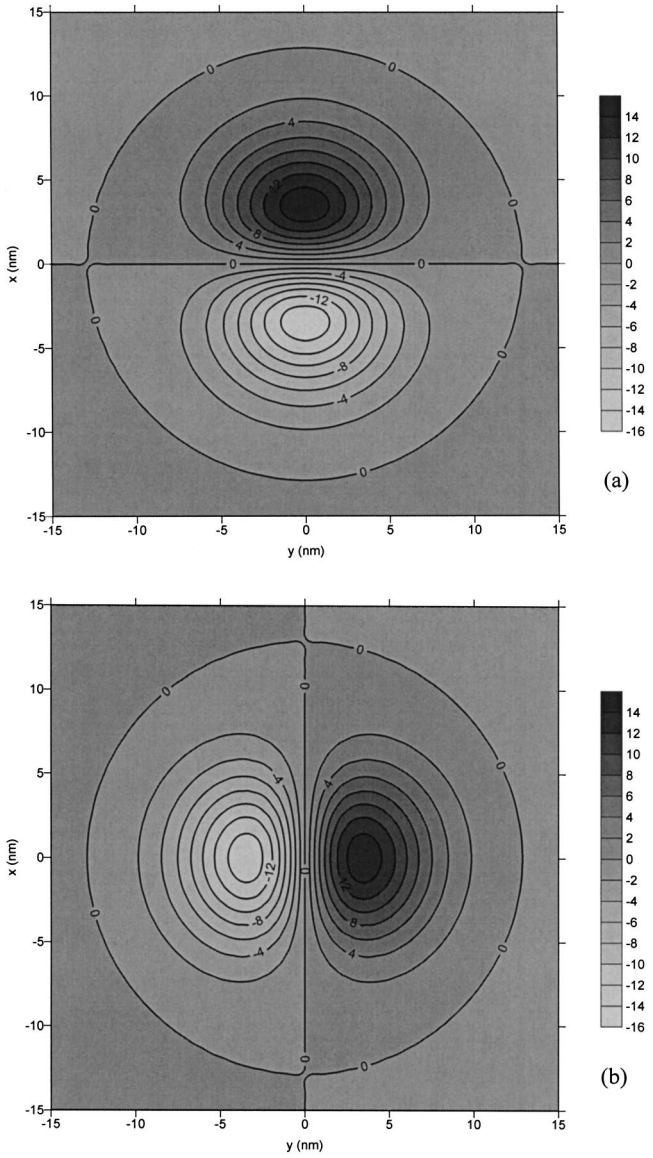

FIG. 5. (a) Contours of the horizontal electric field E_x ($\times 10^7$ V/m) on the surface of AlN (0001) due to a point quantum dot. (b) Contours of the horizontal electric field E_y ($\times 10^7$ V/m) on the surface of AlN (0001) due to a point quantum dot.

reached on the surfaces of AlN (0001) and AlN (1000) are also different, 0.008 versus 0.01. That is, a high-hydrostatic strain is expected if the growth direction in AlN is along the polar direction [i.e., any direction in the plane whose normal is parallel to the (0001) axis].

Plotted in Figs. 3(a) and 3(b) are, respectively, contours of the piezoelectric potential on the surface of substrate AlN (0001) and AlN (1000) due to the same point QD. We remark that while the contours of the piezoelectric potential on the surface of substrate AlN (0001) are again completely rotationally symmetric about the z axis, those on the surface of substrate AlN (1000) show a completely different and special feature. The distribution of the piezoelectric potential on the surface of AlN (1000) is symmetric about the x axis [i.e., the (0001) axis] and antisymmetric about the y axis. Another interesting feature is that the magnitude of the piezoelectric potential on the surface of substrate AlN (0001) is much larger than that on the surface of the corresponding substrate AlN (1000), i.e., 0.81 versus 0.27 V. While the maximum value in AlN (0001) is reached at the center of the surface (i.e., exactly above the point QD), the minimum and maximum values (both with equal magnitude) in AlN (1000) are reached at two points on the x axis, symmetrically located on each side of the y axis. Again, this feature is different from that on the surface of the substrate GaAs.[20]

Figure 4 shows contours of the vertical electric-field E_z on the surface of substrate AlN (0001). The distribution is completely rotationally symmetric about the z axis, with a maximum value of 11×10^7 V/m at the center of the surface. Notice that on the surface of substrate AlN (1000), E_z is identically zero.

Figures 5(a) and 5(b) depict, respectively, contours of the horizontal electric components E_x and E_y on the surface of substrate AlN (0001). We observe that the electric components E_x and E_y are antisymmetric with respect to the y and x axes, respectively, and show similar features, a result of the material symmetry (That is, by rotating one of them $\pi/2$ around the z axis gives the result for the other). We also notice that the horizontal electric-field E_h, defined as $E_h = \sqrt{E_x^2+E_y^2}$, is rotationally symmetric with its maximum value being reached in an annular zone. The maximum value of E_h is equal to that in the electric-field E_x or E_y with a value of 15×10^7 V/m, which is about 50% larger than that in E_z. We further remark that both the horizontal and vertical electric fields on the surfaces of AlN (0001) are in the order of 10^8 V/m, a feature might be useful in the study of the Stark shift.[22,23]

Finally, Figs. 6(a) and 6(b) show, respectively, contours for the electric-fields E_x and E_y on the surface of substrate AlN (1000). It is noted that while E_x is symmetric with respect to both the x and y axes, E_y is antisymmetric with respect to them. For E_x, a minimum of -11.7×10^7 V/m is reached at the center, and two equal maxima of 4.1 $\times 10^7$ V/m on each side of the x axis; For E_y, the two

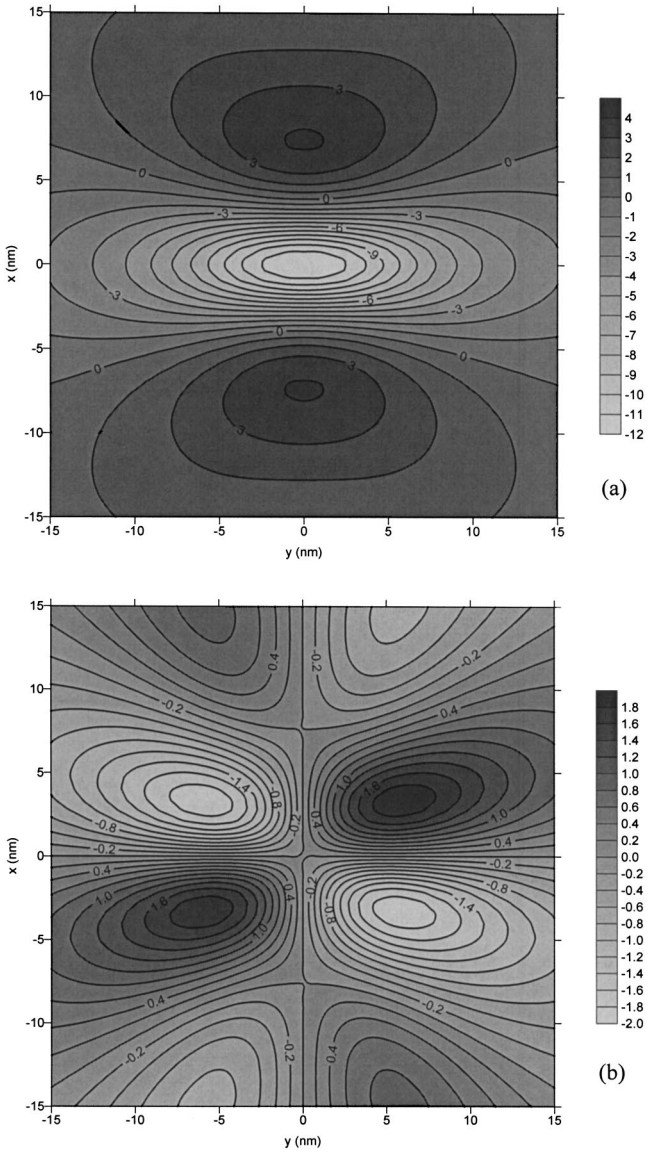

FIG. 6. (a) Contours of the horizontal electric field E_x ($\times 10^7$ V/m) on the surface of AlN (1000) due to a point quantum dot. (b) Contours of the horizontal electric field E_y ($\times 10^7$ V/m) on the surface of AlN (1000) due to a point quantum dot.

maxima and minima have equal amplitude of 2.0×10^7 V/m, located in the four different quadrants on the surface. Since the magnitude of E_x is much larger than that of E_y, the horizontal electric-field E_h follows a similar distribution as E_x, but with slightly changed shapes in certain locations due to the contribution from E_y.

IV. CONCLUSIONS

In this article, a recently derived three-dimensional Green's function in anisotropic and piezoelectric half space has been further applied to study the QD-induced elastic and piezoelectric fields on the surface of an AlN semiconductor substrate with two different growth orientations. The two different growth orientations are the AlN (0001) growing along the (0001) axis, and the AlN (1000) growing along the polar direction [i.e., a direction normal to (0001) axis]. For an InN QD, modeled as a point source, with a volume $v_a = 4\pi R^3/3$ where $R = 3$ nm and the typical misfit strains, at a depth $h = 10$ nm below the surface, certain interesting features have been observed: First, while on the surface of substrate AlN (0001), the hydrostatic strain, piezoelectric potential, vertical electric field and horizontal electric-field (E_h) components are completely rotationally symmetric with respect to the z axis, those on the surface of substrate AlN (1000) are not. Second, a hydrostatic strain as large as 0.01 and 0.008 can be reached, respectively, on the surface of AlN (1000) and the surface of AlN (0001). Third, the piezoelectric potential on the surface of substrate AlN (0001) is much larger than that on the surface of AlN (1000) (0.8 versus 0.3 V). Finally, large horizontal and vertical electric fields, in the order of 10^8 V/m, can be induced on the surface of AlN. We expect that these typical results will be useful in the future study of QD structures, both experimentally and numerically.

ACKNOWLEDGMENT

This research is in part supported by The University of Akron (E. P.).

[1] D. Bimberg, M. Grundmann, and N. N. Ledentsov, *Quantum Dot Heterostructures* (Wiley, New York, 1998).
[2] M. Grundmann, O. Stier, and D. Bimberg, Phys. Rev. B **52**, 11 969 (1995).
[3] T. Benabbas, P. Francois, Y. Androussi, and A. Lefebvre, J. Appl. Phys. **80**, 2763 (1996).
[4] S. Kret, T. Benabbas, C. Delamarre, Y. Androussi, A. Dubon, J. Y. Laval, and A. Lefebvre, J. Appl. Phys. **86**, 1988 (1999).
[5] A. E. Romanov, G. E. Beltz, W. T. Fischer, P. M. Petroff, and J. S. Speck, J. Appl. Phys. **89**, 4523 (2001).
[6] V. Holy, G. Springholz, M. Pinczolits, and G. Bauer, Phys. Rev. Lett. **83**, 356 (1999).
[7] A. D. Andreev, J. R. Downes, D. A. Faux, and E. P. O'Reilly, J. Appl. Phys. **86**, 297 (1999).
[8] C. Pryor, J. Kim, L. W. Wang, A. J. Williamson, and A. Zunger, J. Appl. Phys. **83**, 2548 (1998).
[9] Y. Kikuchi, H. Sugii, and K. Shintani, J. Appl. Phys. **89**, 1191 (2001).
[10] D. A. Faux and G. S. Pearson, Phys. Rev. B **62**, R4798 (2000).
[11] J. R. Downes, D. A. Faux, and E. P. O'Reilly, J. Appl. Phys. **81**, 6700 (1997).
[12] J. H. Davies, J. Appl. Phys. **84**, 1358 (1998); Appl. Phys. Lett. **75**, 4142 (1999).
[13] G. S. Pearson and D. A. Faux, J. Appl. Phys. **88**, 730 (2000).
[14] E. Pan and B. Yang, J. Appl. Phys. **90**, 6190 (2001).
[15] E. Pan and F. G. Yuan, Int. J. Solids Struct. **37**, 5329 (2000); E. Pan, Proc. R. Soc. London, Ser. A **458**, 181 (2001).
[16] J. Singh, *Physics of Semiconductors and Their Heterostructures* (McGraw-Hill, New York, 1993).
[17] B. Jogai, J. Appl. Phys. **88**, 5050 (2000).
[18] B. Jogai, J. Appl. Phys. **90**, 699 (2001).
[19] E. Pan, J. Appl. Phys. **91**, 3785 (2002).
[20] E. Pan, J. Appl. Phys. **91**, 6379 (2002).
[21] J. F. Nye, *Physical Properties of Crystals* (Clarendon, Oxford 1985).
[22] S. Sanguinetti, M. Gurioli, E. Grilli, M. Guzzi, and M. Henini, Thin Solid Films **380**, 198 (2000).
[23] A. Patane, A. Levin, A. Polimeni, F. Schindler, P. C. Main, L. Eaves, and M. Henini, Appl. Phys. Lett. **77**, 2979 (2000).